THE CALIBRATION OF SEGMENTED GAMMA SCANNERS USING ROD SOURCES

S. Croft, R.D. McElroy
Canberra Industries, Inc.
800 Research Parkway, Meriden, Connecticut, 06450, USA.

ABSTRACT

The Segmented Gamma Scanner (SGS) is a widely applied instrument for the assay of suitable radionuclides in low-density radioactive waste drums. The approach involves an axial scan of the item as it is rotated, using a collimated high-resolution gamma spectrometer. A transmission source is frequently employed to determine the energy dependent transmission factor across each layer.

The calibration of the SGS is based on the assumption of a uniform radionuclide distribution, along with matrix homogeneity across each segment. To reduce the time and effort involved in experimentally determining the calibration parameters, a common practice is to simulate uniform source/matrix conditions by inserting an array of 6 or 7 mixed nuclide rod sources into channels placed in simple materials that cover the expected density range.

Errors introduced by the approximation of the uniform source distribution by a fixed pattern of multiple ideal line sources are examined. We show that placing the rods at the centroid of equal volume cylindrical shells provides an excellent analog. Additional factors such as the net energy dependent effect on the apparent specific emission rate at the detector due to the finite self attenuation suffered in the structure of the rods, including the associated re-entrant channels, and the displaced matrix material are considered. We present a table of correction factors for common nuclides and test matrices. It is concluded that the multi rod approach can be used to high accuracy over an extremely broad range of transmission factors.

INTRODUCTION

Transmission corrected Segmented Gamma Scanning is a well-known and widely applied method for the qualification of γ-emitters in waste drums [1, 2]. Several hundred Segmented Gamma Scanners are currently in routine use throughout the world making them one of the most popular non-destructive assay tools. The SGS technique combines quantitative high-resolution γ–spectrometry with an axial scan of the item as it is rotated to produce an estimate of the activity segment by segment. Matrix attenuation corrections, for each segment, are derived from diametrical transmission factors measured using an external multi-energy transmission beam. The fundamental assumptions underpinning the application of the SGS are that within each segment the matrix material and density is constant and homogeneous and furthermore that the distribution of activity is uniform in the matrix. In practice neither of these assumptions is satisfied perfectly. This is why the drum is continuously rotated for an integral number of rotations per segment during the counting period. During the Transmission measurement the rotation results in an approximate averaging of matrix inhomogeneities while in Emission mode it approximately evens out inverse square and attenuation variations due to a non-uniform activity distribution. As a matter of pragmatism the choice of scanning pattern is a trade off between accuracy and precision. Performing a scan with high spatial definition in principle may result in a more accurate assay result by adhering more closely to the underlying assumptions but it will also take longer so that given time constraints detection limits or throughput performance will be impaired. Because of this, typically only between 8-16 segments are used and a slot collimator some 4" tall by 10" wide by 8" long located perhaps only 4" from the drum wall would be a reasonable compromise. Because such an arrangement defines a broad field of view extending to segments above and below the one nominally selected during the axial scan, there is also an implicit assumption that the axial variation of the waste is smooth and gradual. Recall too that the Transmission beam may only be a fraction of the height of the segments being used, so that the axial coverage, even within a segment, is limited.

Given the fundamental assumptions of the SGS technique and the general method of practical implementation, the method is most reliable when applied to items with homogeneous matrix and uniform activity distributions, or, to items of low-to-medium gross density (≤ 0.5 g.cm^{-3}, say in the case of 200L drum; reference [1] covers diametrical

transmission factors of 1% or greater) known to have modest variation or alternatively known to have sufficient randomness that the averaging processes introduced by the scanning procedure are effective.

In practice there is ample empirical evidence that the SGS approach works remarkably well across a wide range of assay conditions and is sufficient to meet a broad range of regulatory and operational needs. Solid items, say, represent a severe case of inhomogeneity but are often only contaminated on the surfaces so that frequently this kind of violation of the SGS assumptions again gets smoothed out. The net result is that provided there are at least a few random 'pockets' (or 'hot regions') of activity in the drum, perhaps as few as 3-5, the SGS approach works well.

In accordance with the underlying assumptions and operational experiences it is, therefore, conventional to calibrate SGS instruments under conditions of homogeneous matrix and uniform activity. Allowance for 'point-source' effects is then accommodated by the Total Measurement Uncertainty. To reduce the time and effort involved in experimentally determining the calibration parameters, a common practice is to simulate uniform conditions by inserting an array of 6 or 7 mixed nuclide rod sources into channels placed in simple, often stable and self-supporting, homogeneous materials that cover the expected density range. The use of rods simulates a uniform axial distribution rather well. The radial disposition of the rods is chosen to approximate a uniform radial distribution (in terms of per unit volume).

In this paper we address the following questions:

1. how well does a fixed pattern of 6 or 7 ideal line sources mimic a uniform activity distribution?

and

2. what is the net energy dependent effect on the apparent specific emission rate at the detector due to the finite self attenuation suffered in the structure of the rods, including the associated re-entrant channels, and the displaced matrix material?

This is all part of ensuring that the calibration is accurate and well understood. It is important to bear in mind, however, that the uncertainties associated with measuring actual waste drums may, of course, be much larger than the uncertainty associated with the calibration procedure. The matrix and activity distributions will seldom be ideal. Even the variation in fill height introduces end effects bias. For the purposes of discussion we describe a particular calibration geometry although the method is quite general.

Method

The live-time corrected full energy peak count-rate corrected for continuum and peaked background may be expressed as:

Rate = cal_coeff $\cdot$ A $\cdot$ f_{lump} $\cdot$ f_{matrix}

where A is the activity of nuclide present; f_{lump} is the average self attenuation factor suffered in any 'lumps' of nuclide present (assumed to be unity in the present discussion); cal_coeff is the specific count-rate calibration coefficient for the nuclide uniformly and dilutely dispersed throughout an empty drum; and f_{matrix} is the attenuation caused by the matrix within the drum.

Rearranging for A:

A = (1/cal_coeff) $\cdot$ CF_{lump} $\cdot$ CF(T) $\cdot$ Rate

where CF_{lump} is the lump correction factor given by (1/f_{lump}) and CF(T) = 1(f_{matrix}) is the gross matrix correction factor corresponding to the rotationally averaged diametrical transmission factor T.

The form of CF(T) may be extracted by empirically fitting to calibration data although this is rarely done where measured transmission data is available. Instead a semi-empirical form is routinely used. That is, CF(T) is typically

calculated from a semi-empirical relationship for a homogeneous cylinder containing a uniform distribution of activity. The performance, however, may be checked by comparison to direct experimentation. The observed response must be corrected for matrix attenuation. In the case of the Volume Weighted Average (VWA) response (which assumes the activity per unit volume is constant) this raises the question of how well 6 or 7 rod sources embedded into a test matrix, according to some loading pattern, represents a uniform activity distribution. In particular, one must consider whether there is a matrix density bias introduced by the method. The possibility that the matrix correction factor vs. measured transmission curve derived from the system characterization data exhibits a density bias comes about for the following reasons. First one must consider whether an array of ideal line sources, which when rotated sweep out shells of activity, adequately mimic a uniform distribution. Second the rod sources and the uPVC re-entrant source tubes into which they are placed (see later) can not be regarded as ideal line sources. They (i) displace matrix material and (ii) have finite self-attenuation. It is important therefore to consider relative γ-attenuation between an ideal line source at the center of the displaced matrix and the actual rod in the uPVC guide tube as will be described below.

By inspection the difference between a calibration using a uniform drum and a calibration using rod sources can be treated in two steps. The observed count-rate, R_{obs}, measured in the matrix simulant must be corrected by two factors which can be estimated separately in order to estimate the volume weighted average rate, R_{VWA}.

$$R_{VWA} \quad = \quad CF_{geom} \cdot CF_{pert} \cdot R_{obs}$$

The first factor, CF_{geom}, accounts for any mismatch between 6 or 7 shell sources and an ideal uniform distribution. The second factor, CF_{pert}, accounts for the fact that the rods are not ideal line sources running along the center of a cylinder of matrix. Rather a cylinder of matrix has been cut away and replaced by a guide tube and the rod with air gaps in between.

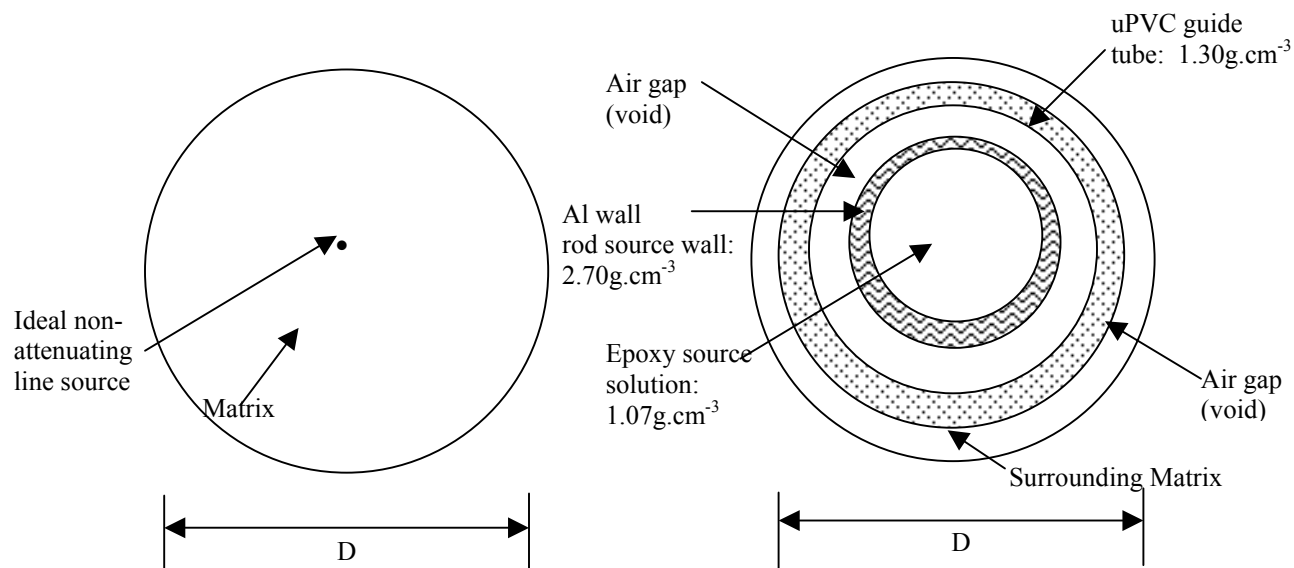The situation is illustrated below; the details used for modeling of the materials are also summarized:

Fig. 1.

In the following segments we describe the rod sources, the test drums and the deployment of rods within them. Given this background, we go on to describe how the matrix attenuation factors introduced above have been evaluated.

Rod Sources

In this section we describe the construction of the rod sources [manufactured by North American Scientific Inc, Jeff Wagner, Priv. Comm. 2002; and Michael Hill, Priv. Comm. 2005] sufficient to calculate the self-absorption taking place in them. The arrangement of rods in the drum is intended to simulate a uniform distribution of activity.

The mixed nuclide solutions used to make the sources are prepared by dispensing gravimetric aliquots of individual calibrated solutions into a master batch. An aliquot of the master batch was then gravimetrically transferred to each standard. The nuclide solutions were calibrated using a HPGe whose efficiency as a function of gamma ray energy had been established and verified through ongoing inter-comparisons with the US National institute of Standards and Technology.

The activity is uniformly distributed in an epoxy matrix with a density of 1.07g.cm^{-3} and cast directly into a 6.35mm (0.250") outer diameter by 830mm (32.7") long aluminum tube with 0.89mm (0.35") thick walls. The active diameter is, therefore, 4.57mm (0.18"). Both ends of the tube are capped with 2mm (0.08") plugs to give an active length of 826mm (32.5"). The length was chosen to closely match that of the nominal drum fill height (33") with an allowance for clearance in the eventuality of upward bowing of the drum base. An alternative diameter rod has also been widely used by us (see summary of matrix specifications in the Results section).

The source matrix, epoxy resin, appears to have a composition of Amidoamine (CAS-68443083) 80wt% and Tetraethylenepentamine, TEPA, (CAS 112-57-2) 20wt%

The composition of Amidoamine resin seems to be proprietary information. It is referenced as being a component in the hardener component of two component epoxy resins. Amines, polyamines and fatty acids are generically formed by replacing one or more of the hydrogens of the ammonia molecule by an organic radical, e.g. $(CH_3)_2$-H-H

TEPA, $C_8H_{23}N_5$, is referenced as being a component of epoxy resin. Another major constituent is Bisphenol a diglycidal ether resin, DGEB, $C_{21}H_{24}O_4$.

In general 'two part repair compound epoxy compounds' appear to have quite complex and variable chemical compositions and can include silica, carbon, and a number of organic compounds. For the present purposes it is considered sufficient to model any attenuation in the source by representing the epoxy matrix by Perspex (PMMA) with an effective density of 1.07g.cm^{-3}.

Rod uniformity is checked by counting on a NaI(Tl) detector. A collimator is used to divide the line sources into 10 mm increments. The uniformity is determined by calculating the Maximum Average Deviation from the Mean (MADM) of the 10 mm sections. Each line source has a typical MADM of less than 5%. To verify this manufacturing process, each rod source was collimated and counted using a high purity Germanium detector. The resulting count rates of each rod source were within 5% of the average. To clarify the meaning of MADM: the rod is measured in 10mm long sections; the average is determined; the segment which deviates most from the mean is determined and expressed as a percentage. Thus, the variation of one segment to the next is actually much better than this. On this basis axial uniformity is assumed for practical waste applications.

The activity of each nuclide in each of the rods is also closely matched across a given rod set. The original requirement to be within 3% of the average has been translated such that the certificated activity of each rod is within 5% of the set average at the 99% confidence level.

Drum Data

The surrogate matrices were prepared as disks that can be stacked into standard waste drums. Depending on origin small differences exist between drums used on different sites. Typically internal diameters lie in the range of 22.25"–24.5". We shall present here results for what we refer to as DRP drums. Table I gives a summary of the drum model. In the present paper we adopt a matrix radius of 11.16" and an internal fill height of 33" equating to a

volume of 211.6L. Results for the 17C and 17H drums, see Table 1, using only 6 rods have also been shown to produce very similar overall performance. Details can be provided on request.

Holes were cut into the disks to accept the rod sources. The holes were lined with uPVC (CPVC, C_2H_3Cl) FlowGuard Gold Charlotte drinking water pipes 33" long. The pipes had an internal diameter of approximately 0.47" and an outer diameter of 0.63". In the case of the sand filled drum the reentrant source guide tubes (uPVC pipes) are set into ¾" particleboard at the top and bottom thus the height of the sand is only 31.5" rather than 33". Also, the sand occupies the full radial extent of the drum (11.25") including the rolling hoops (taken as half circle in cross section with a radius of 0.59"). In the case of the empty drum a set of uPVC pipes is still used with the individual rods held together by thin Perspex centering disks at the top and bottom, heavily cut-away to minimize the weight.

Table I. Summary of Drum Models

Drum Type		DRP	17C and 17H
Hole in Matrix,	Diameter	0.750"	0.906"
uPVC Tube,	OD	0.630"	0.875"
	ID	0.469"	0.750"
	Wall	0.0805"	0.0625"
Source Rod,	OD	0.250"	0.375"
	Al wall thickness	0.035"	0.035"
Epoxy (by Difference)	Diameter	0.180"	0.305"
Matrix,	Diameter	22.32" (567.0mm)	22.25"
Homogenized rod assembly density over volume of matrix removed		0.628g.cm^{-3}	0.626g.cm^{-3}

Rod Placement

In order to approximate a uniform activity distribution using a set of n calibrated rod sources of equal strength inserted parallel to the drum axis, imagine the cross-section of the drum being divided into n equi-volume annuli. We choose to place a rod at the radius which divides each volume element into half – that is at the centroid of activity for a uniform activity per unit volume distribution. Denoting the radius of the ith rod by s_i, this gives:

$$(s_i)^2 \quad = \quad (i - \tfrac{1}{2}) \cdot a^2/n , \quad i = 1 \text{ to } n$$

where a is the internal radius of the drum – the radius of the waste matrix.

Note that we (would generally prefer to and have for the DRP set) avoid placing a rod at the center of the matrix since this will disturb the transmission beam all the time. Due to manufacturing tolerances the matrix simulant will not fill the whole drum diameter nor will it spill into the rolling hoops but these effects are small and can be allowed for in the calculations. To be physically realizable then $(a-s_n)$ must be greater than the effective source rod radius, b, including the uPVC pipe and full extent of the associated matrix removed. That is:

$$n_{max} < (\tfrac{1}{2}) / (1-[1-(b/a)]^2)$$

In practical terms for nominal 200L (55 US gal) drums (b ~ 0.32", a ~ 11.1" from the Drum Model Table) this limits the number of rods to about 8. Historically 6 rods have been used, sometimes 7, while for 400L drums (~28" I.D.) we have used 7 rods. This choice was based on the assumption that the more rods the better would be the uniform approximation especially as the drum density increases (strictly speaking as the transmission factor decreases – since the transmission is matrix, density and energy dependent).

Note, this general approach is long established [see e.g. 3-5] for the calibration of the Canberra Quantitative and Qualitative (Q^2) Low Level Waste System. For general-purpose applications drum sets with nine vertical holes [see the 17C and 17H specification] are routinely supplied. One hole (designated number 1) lies along the central axis,

six others (2, 3, 4, 5, 6, 9) are located at the centers of size equal-volume annuli and two others (7 & 8) are placed near the outside of the drum. Hole number 5 represents the position close to the uniform distribution. The central tube is included as the explicit expression of lowest response in cases were radial scans are required. Extra holes are included near the drum surface because the efficiency is highest and most rapidly changing in this region in the use of dense drums. Measurements with an individual rod in each hole separately permits axially averaged radial profiles to be determined and used explicitly to calculate radial averages. This is the approach taken by Bruggeman et al [5].

Although in the present scheme all rods carry equal weight of course the outermost rods will dominate the response, especially when the penetrability of the matrix is low. Therefore, the rods closest to the drum edge should be those closest to the mean of the aggregate activity of the (nominally matched) set.

The holes are arranged in a pattern so that when viewed along a diameter no more than one hole intersects the transmission beam and is aligned with the detector. For example, for a 7 hole pattern an angular pattern of 0°, 45°, 90°, 135°, 202.5^o, 247.5^o and 292.5^o would be acceptable.

In the special case of n = 1 the above formula would place the rod at $s_1 = (a/\sqrt{2}) \sim 0.71a$. Clearly, on a case by case basis one could, if one were so minded, calculate the position of a single rod position to replicate the VWA response more accurately than this. The motivation for so doing might be to create a sealed, check calibration drum for routine use at a minimal cost. We state here, without further discussion, that a single rod can provide a 'reasonable' approximation to the uniform source distribution if properly placed. A good, general single rod position is about 80-85% of the drum radius.

The present work is complementary to the detailed point kernel study of a 7 rod calibration of the Q^2 carried out by Liang et al [4]. The modeling performed by these workers is quite powerful but the results are presented graphically and not readily accessible. They present an interesting discussion on optimizing rod position and also propose a 3 rod scheme. This is intermediate in complexity between the 6/7 and 1 rod concepts discussed already.

An obvious extension to the laborious scanning of a point source [6] to generate type test style response function data in support of spatial uncertainty analysis is the use of a rod source set combined with matrix specific calculated correction factors. In essence the experimental results are used to peg the absolute response and the calculational tool is used to calculate ratios used to generate small, relative, refinements or adjustments. In this way one benefits from the advantage of rapid experiments with minimal impact on ultimate calibration accuracy. A detailed calculational tool permits the experimental results to be scaled to different drum sizes, matrix densities outside the range considered experimentally, and to explicit collimator and scanning scenarios. The application of mathematical calibration tools is becoming more widespread in the waste assay community but further discussion is beyond the present scope.

Evaluation

The treatment given here is pedagogic in nature and in the spirit of the established Parker formalism to highlight the physical principals involved. In order to present a generic discussion we limit ourselves to the case of the Far Field Approximation (FFA). The rods are treated as independent of each other. Because this approach ignores other geometrical effects such as the drum-to-detector separation, which varies from system to system and also matrix absorption, the emission centroid selected is not expected to coincide with the apparent or effective point of emission from the point of view of detection efficiency. In fact, this changes with γ–ray energy and matrix. Therefore, we use fixed rod positions for all calibration matrices and elect to apply an appropriate and system specific scaling factor at the end if needed. The evaluation has been coded into a spreadsheet so that changes in matrix density, rod positions, rod dimensions, hole details etc. can be entered easily and new tables generated almost immediately. This is a major advantage over detailed modeling using a general-purpose point kernel, Monte Carlo or similar transport codes.

The matrix attenuation, at a given γ–energy, for an array of ideal line sources rotated to form an array of cylindrical surface shells was calculated by summing over i the term:

$$(A_i/A) \cdot f_{shell}\,(T, s_i/a)$$

where A_i is the activity of the ith source, A being the total activity of the set and f_{shell} is the attenuation factor for a shell at fractional radius (s_i/a) in a matrix with a diametrical transmission factor of T. In the present case (A_i/A) was set equal for all i. The function f_{shell} was evaluated by simple numerical integration of the algebraic form using an angular spacing of 0.125^o.

For a uniform source distribution the matrix correction factor is of the order of (borrowing from Jack Parker [7-9]):

$$CF(uniform) = \ln(1/T^\kappa) \,/\, (1-T^\kappa)$$

where κ is a geometrical factor that can be thought of (at least for low density waste) as the factor by which the diameter must be multiplied by in order to obtain the mean path length of the emerging photons out of the plane of the uniform disk. On this basis the value of κ is expected to take on a value close to $\kappa_L=(8/(3\cdot\pi))$ or 0.849 in the case of lightly attenuating drums. For highly attenuating drums we expect the value of κ to be close to $\kappa_H=(\pi/4)$ or 0.785. In practice κ may be treated as a free parameter to be determined empirically to best fit a body of experimental data although the geometrical mean value of 0.816 also works well.

In the present work we have used a variation of Parker's formula, introduced by Croft et al [2] to estimate CF(*uniform*). We have found that this reproduces the Far Field Approximation (FFA) results very well. This has been confirmed by comparison with the procedure for calculating the attenuation of disk sources set out by Dickens [10]. The proposed formula reproduces volume weighted average results to within a few percent for transmissions greater than 0.001 which covers the range of normal practical application. Another reason for choosing the Parker form is because this is the form embodied as an option into most SGS implementations. The correction factor is equal to the reciprocal of a weighted average matrix attenuation factor where the weights are chosen to smoothly join the low- and high-density approximations (the two κ-values referred to earlier). Thus:

$CF(uniform) \approx 1/f$ where $f = (f_L/x_L+x_H\cdot f_H)/(1/x_L+x_H)$
and $x_L=\kappa_L\cdot(\mu/\rho)\cdot\rho\cdot D$; $x_H=\kappa_H\cdot(\mu/\rho)\cdot\rho\cdot D$; $f_L=(1-\exp(-x_L))/x_L$; $f_H=(1-\exp(-x_H))/x_H$

Inelastic photon interaction data for the elements and compounds were generated from the compilation Berger et al [11]. The total interaction cross section excluding the coherent scattering contribution was used because we are only interested in collisions that remove the photon from the full energy peak (FEP). Coherent scattering merely re-directs the photon, and, to first order, in-scatter and out-scatter contributions cancel.

The 'normal' level of attenuation expected for γ-rays from the ideal line source in the surrounding matrix is f_O. The corresponding attenuation of a rod source in the uPVC guide tube is f_R. Therefore, the apparent or effective attenuation factor of the rod is:

$$f_{eff} \qquad = \qquad (f_R / f_O)$$

f_{eff} is the attenuation factor over and above that (built into the calibration method) of an ideal line source placed in the drum matrix. This is obvious by considering light matrices where $f_O \sim 1$, whereas on the other hand, f_R remains <1 for this case because the epoxy/Al-tube/uPVC pipe combination has an effective density greater than zero taken over the volume of matrix removed (refer to the materials Table).

If $f_{eff} < 1$, then the source is effectively attenuating compared to the ideal line source assumption. At low densities the rod assembly is a net self-attenuator by up to 17% or so for the 60keV line from [241]Am but it flips to greater than unity for higher drum matrices.

For the ideal line source embedded in a cylinder of matrix of radius b, f_O, in the FFA, is given simply be the exp(-$\mu\cdot$b) where μ is the linear attenuation coefficient of the matrix material. This is the simple slab or window form factor.

For the finite rod we have $f_R = f_{epoxy} \cdot f_{Al} \cdot f_{uPVC}$ where the attenuation in the Al jacket and in the uPVC guide tube are evaluated using the window form. The attenuation factor for the epoxy, f_{epoxy}, was evaluated using the modified Parker form as described above.

Results

For illustrative purposes we consider here results for a range of calibration nuclides covering the principal ones of routine interest. These include [241]Am, [133]Ba, ^{137}Cs and ^{60}Co that commonly form one mixed-nuclide rod set. In addition the nuclide [152]Eu has been included which can be used alone or in combination as an alternative to the AmBaCsCo mix. Taken together this set of nuclides covers the energy range from 60keV to 1408keV. Out of interest, the principle lines used for the quantitative waste assay of [235]U and [239]Pu have also been included. Gamma energies were taken from [12].

The matrix materials considered are listed in Table II. These materials represent a wide range of waste types from uncompacted light wastes (0.1 – 0.3 g.cm^{-3}), light compacted wastes (0.8 g.cm^{-3}), through heavy wastes containing substantive solids (~1.5 – 3 g.cm^{-3}).

Table II. Summary of Matrix Specifications

Matrix id	Description	Bulk Density (g.cm^{-3})	Material representation
MT	Empty	0.000	Null or void
FM	Foam	0.0192	Low density expanded polyurethane foam. Polyurethane has a variable composition. Here we take ($C_{10}O_3N_1H_{14}$) as typical.
MW	Mineral Wool	0.112	Made by mixing stone with molten slag from blast furnaces and blowing steam through it, the composition is consequently difficult to estimate. We 'guestimate' the following composition expressed in wt.%. H (0.6) : O (45.1) : Mg (1.7) : Al (8.9) : Si (21.1) : Ca (20.5) : Fe (2.1)
HS	Homosote	0.438	Softboard or fiberboard represented by cellulose ($C_6H_{10}O_5$)
PB	Particle Board	0.681	Composition assumed to be 90wt% cellulose ($C_6H_{10}O_5$) and 10% lignum binder ($C_{41}H_{32}O_6$)
PX	Perspex	1.195	Lucite, Plexiglas, Polymethylmethacrylate (PMMA) which has a chemical formula of ($C_5H_8O_2$)
SD	Sand	1.496	Fine industrial grade 'Quikrete' silicon dioxide (SiO_2) blasting sand

The primary results for the DRP drum geometry are summarized in Table III. For each γ-energy calculated parameters are listed by matrix: T is the transmission factor of the matrix across the diameter; f_{eff} is the net attenuation effect in the rod over that of the matrix displaced; R is the ratio of the gross matrix attenuation factor calculated in the shell approximation to that evaluated according to the modified Parker form and the product $f_{eff}.R$ represents the overall deviation of the rod approximation from the ideal uniform simulation. For the empty drum the net effect of the rod representation is that self-absorption with the rods and uPVC pipes dominates. The empty drum (e.g. a drum filled with radioactive gas) is not a realistic practical case and so these results are not of much consequence (sacrificial empty drums are sometime checked after use prior to compaction or disposal but these can be treated as a unique stream). For the foam, mineral wool, Homosote and particleboard matrices the rod approximation is seen to be excellent overall. For these cases the transmission factors are typically above about 0.1% and the overall deviations are within a few percent. For the two denser matrices considered, Perspex and sand, the deviations are somewhat larger, up to about 25%, although still reasonable given the overall measurement accuracy achievable of such dense items with transmission factors that are only a small fraction of a per cent in many cases. We note that the predominate reason for the deviations from unity for these two matrices is not the

break down of the shell approximation but is rather due to the differential attenuation between the rod and pipe assembly and the displaced matrix. Appropriate calculated compensation factors can, of course, be applied as needed.

Although we have elected here to tabulate the results for each γ–line by matrix we observe that they could also be ordered by diametrical transmission factor to define a single curve. Strictly this is true with the exception of the sand matrix, where there is no air gap between the uPVC pipe and matrix.

Table III. Summary of Results for the DRP Drum Geometry

Gamma Energy (MeV)	Nuclide	MT: 0.00 g.cm^{-3}				FM: 0.0192 g.cm^{-3}				MW: 0.112g.cm^{-3}				HS: 0.438 g.cm^{-3}				PB: 0.681 g.cm^{-3}				PX: 1.195 g.cm^{-3}				SD: 1.496 g.cm^{-3}			
		T	f_{eff}	R	f_{eff}.R	T	f_{eff}	R	f_{eff}.R	T	f_{eff}	R	f_{eff}.R	T	f_{eff}	R	f_{eff}.R	T	f_{eff}	R	f_{eff}.R	T	f_{eff}	R	f_{eff}.R	T	f_{eff}	R	f_{eff}.R
0.0595	^{241}Am	1	0.837	1.000	0.837	0.822	0.843	1.000	0.843	0.136	0.896	0.979	0.877	1.12E-02	0.974	0.972	0.946	9.58E-04	1.058	0.975	1.031	4.41E-06	1.267	0.968	1.227	4.33E-09	1.442	0.943	1.359
0.0810	^{133}Ba	1	0.875	1.000	0.875	0.834	0.881	1.000	0.881	0.263	0.916	0.987	0.904	1.63E-02	1.005	0.971	0.976	1.65E-03	1.086	0.974	1.058	1.14E-05	1.283	0.970	1.245	3.28E-07	1.334	0.960	1.281
0.2764	^{133}Ba	1	0.923	1.000	0.923	0.880	0.927	1.000	0.927	0.497	0.945	0.997	0.942	5.63E-02	1.017	0.973	0.989	1.13E-02	1.073	0.972	1.043	3.37E-04	1.208	0.975	1.177	8.86E-05	1.201	0.974	1.170
0.3029	^{133}Ba	1	0.926	1.000	0.926	0.884	0.930	1.000	0.930	0.506	0.947	0.997	0.945	6.21E-02	1.016	0.973	0.989	1.32E-02	1.071	0.971	1.040	4.42E-04	1.200	0.975	1.170	1.24E-04	1.193	0.974	1.163
0.3560	^{133}Ba	1	0.930	1.000	0.930	0.890	0.934	1.000	0.934	0.529	0.950	0.998	0.948	7.21E-02	1.016	0.974	0.989	1.67E-02	1.067	0.971	1.036	6.64E-04	1.189	0.975	1.159	2.14E-04	1.180	0.975	1.151
0.3838	^{133}Ba	1	0.932	1.000	0.932	0.893	0.936	1.000	0.936	0.539	0.952	0.998	0.950	7.77E-02	1.016	0.974	0.989	1.87E-02	1.065	0.971	1.035	8.70E-04	1.181	0.975	1.151	2.74E-04	1.175	0.975	1.145
0.6617	^{137}Cs	1	0.945	1.000	0.945	0.914	0.948	1.000	0.948	0.612	0.961	0.999	0.960	1.31E-01	1.012	0.978	0.990	4.25E-02	1.051	0.972	1.022	3.56E-03	1.143	0.973	1.112	1.46E-03	1.137	0.974	1.108
1.1732	^{60}Co	1	0.958	1.000	0.958	0.934	0.960	1.000	0.960	0.688	0.970	1.000	0.970	2.13E-01	1.009	0.984	0.994	9.02E-02	1.039	0.975	1.013	1.36E-02	1.107	0.971	1.075	6.88E-03	1.103	0.972	1.072
1.3325	^{60}Co	1	0.961	1.000	0.961	0.938	0.963	1.000	0.963	0.704	0.972	1.000	0.972	2.35E-01	1.009	0.986	0.994	1.05E-01	1.036	0.976	1.012	1.79E-02	1.100	0.971	1.068	9.41E-03	1.096	0.972	1.065
0.1218	^{152}Eu	1	0.898	1.000	0.898	0.848	0.903	1.000	0.903	0.373	0.928	0.993	0.922	2.42E-02	1.018	0.971	0.988	3.05E-03	1.091	0.973	1.062	3.37E-05	1.269	0.973	1.235	4.18E-06	1.274	0.968	1.233
0.2447	^{152}Eu	1	0.920	1.000	0.920	0.876	0.924	1.000	0.924	0.478	0.943	0.996	0.940	4.97E-02	1.018	0.972	0.989	9.35E-03	1.076	0.972	1.046	2.40E-04	1.217	0.975	1.187	6.31E-05	1.209	0.974	1.177
0.3443	^{152}Eu	1	0.929	1.000	0.929	0.889	0.933	1.000	0.933	0.526	0.949	0.998	0.947	7.03E-02	1.016	0.974	0.989	1.61E-02	1.067	0.971	1.037	6.20E-04	1.191	0.975	1.161	1.90E-04	1.183	0.975	1.153
0.4111	^{152}Eu	1	0.934	1.000	0.934	0.896	0.937	1.000	0.937	0.548	0.953	0.998	0.951	8.37E-02	1.015	0.975	0.989	2.11E-02	1.063	0.971	1.032	9.97E-04	1.178	0.975	1.148	3.38E-04	1.170	0.975	1.141
0.4440	^{152}Eu	1	0.936	1.000	0.936	0.899	0.939	1.000	0.939	0.558	0.954	0.998	0.952	9.01E-02	1.015	0.975	0.989	2.37E-02	1.061	0.971	1.030	1.25E-03	1.171	0.974	1.141	4.33E-04	1.164	0.975	1.135
0.7789	^{152}Eu	1	0.949	1.000	0.949	0.920	0.952	1.000	0.952	0.634	0.964	0.999	0.963	1.52E-01	1.011	0.980	0.991	5.34E-02	1.047	0.972	1.019	5.31E-03	1.132	0.973	1.101	2.30E-03	1.127	0.974	1.097
0.8674	^{152}Eu	1	0.952	1.000	0.952	0.924	0.954	1.000	0.954	0.648	0.966	0.999	0.965	1.66E-01	1.011	0.981	0.992	6.16E-02	1.045	0.973	1.017	6.87E-03	1.125	0.972	1.094	3.12E-03	1.120	0.973	1.090
0.9641	^{152}Eu	1	0.954	1.000	0.954	0.927	0.956	1.000	0.956	0.662	0.967	0.999	0.967	1.82E-01	1.010	0.982	0.992	7.07E-02	1.043	0.974	1.015	8.77E-03	1.119	0.972	1.087	4.13E-03	1.114	0.973	1.084
1.0858	^{152}Eu	1	0.957	1.000	0.957	0.931	0.959	1.000	0.959	0.678	0.969	1.000	0.969	2.00E-01	1.010	0.983	0.993	8.19E-02	1.040	0.975	1.014	1.14E-02	1.112	0.972	1.080	5.66E-03	1.107	0.972	1.076
1.0897	^{152}Eu	1	0.957	1.000	0.957	0.931	0.959	1.000	0.959	0.678	0.969	1.000	0.969	2.01E-01	1.010	0.984	0.993	8.22E-02	1.040	0.975	1.014	1.16E-02	1.111	0.972	1.080	5.71E-03	1.107	0.972	1.076
1.1121	^{152}Eu	1	0.957	1.000	0.957	0.932	0.959	1.000	0.959	0.681	0.969	1.000	0.969	2.04E-01	1.010	0.984	0.993	8.45E-02	1.040	0.975	1.014	1.21E-02	1.110	0.971	1.078	6.00E-03	1.106	0.972	1.075
1.2129	^{152}Eu	1	0.959	1.000	0.959	0.935	0.961	1.000	0.961	0.692	0.971	1.000	0.970	2.19E-01	1.009	0.985	0.994	9.38E-02	1.038	0.976	1.013	1.46E-02	1.105	0.971	1.073	7.48E-03	1.101	0.972	1.070
1.2991	^{152}Eu	1	0.960	1.000	0.960	0.937	0.962	1.000	0.962	0.701	0.972	1.000	0.971	2.30E-01	1.009	0.985	0.994	1.02E-01	1.037	0.976	1.012	1.69E-02	1.101	0.971	1.070	8.79E-03	1.097	0.972	1.067
1.4080	^{152}Eu	1	0.962	1.000	0.962	0.939	0.964	1.000	0.964	0.711	0.973	1.000	0.973	2.44E-01	1.008	0.986	0.995	1.12E-01	1.035	0.977	1.011	1.99E-02	1.097	0.971	1.065	1.07E-02	1.093	0.972	1.062
0.1438	^{235}U	1	0.904	1.000	0.904	0.855	0.909	1.000	0.909	0.403	0.932	0.994	0.927	2.88E-02	1.019	0.971	0.989	4.00E-03	1.089	0.973	1.059	5.41E-05	1.258	0.973	1.224	8.96E-06	1.255	0.970	1.217
0.1857	^{235}U	1	0.912	1.000	0.912	0.864	0.917	1.000	0.917	0.443	0.937	0.996	0.933	3.69E-02	1.019	0.972	0.990	5.88E-03	1.084	0.972	1.054	1.07E-04	1.240	0.974	1.208	2.28E-05	1.233	0.972	1.199
0.1293	^{239}Pu	1	0.900	1.000	0.900	0.850	0.905	1.000	0.905	0.385	0.930	0.993	0.924	2.61E-02	1.018	0.971	0.988	3.43E-03	1.090	0.973	1.060	3.86E-05	1.267	0.973	1.232	5.39E-06	1.268	0.969	1.228
0.2036	^{239}Pu	1	0.915	1.000	0.915	0.868	0.919	1.000	0.919	0.454	0.939	0.996	0.935	4.08E-02	1.019	0.972	0.990	6.87E-03	1.081	0.972	1.051	1.40E-04	1.233	0.974	1.201	3.20E-05	1.225	0.973	1.191
0.3328	^{239}Pu	1	0.928	1.000	0.928	0.888	0.932	1.000	0.932	0.519	0.949	0.997	0.947	6.69E-02	1.017	0.973	0.990	1.54E-02	1.068	0.971	1.037	5.80E-04	1.193	0.975	1.163	1.75E-04	1.185	0.975	1.155
0.3751	^{239}Pu	1	0.932	1.000	0.932	0.892	0.935	1.000	0.935	0.536	0.951	0.998	0.949	7.58E-02	1.016	0.974	0.990	1.80E-02	1.066	0.971	1.035	8.13E-04	1.183	0.975	1.153	2.54E-04	1.177	0.975	1.147
0.4137	^{239}Pu	1	0.934	1.000	0.934	0.896	0.937	1.000	0.937	0.549	0.953	0.998	0.951	8.41E-02	1.015	0.975	0.989	2.13E-02	1.063	0.971	1.032	1.07E-03	1.175	0.975	1.146	3.47E-04	1.169	0.975	1.140

CONCLUSIONS

The conventional calibration of an SGS relies on generating a volume weighted average response in homogeneous matrices. The use of rod sources provides for axial uniformity of activity. In this paper we have shown that placing 6 or 7 rods at the centroid of equal volume cylindrical shells provides an excellent analog to a uniform radial distribution (on a per unit volume basis). The effect of the net absorption in the rods and channel has been examined. A table of correction factors for common nuclides and test matrices was given for the case of nominal 210L / 55 US gal drums.

It is concluded that the multi-rod approach can be used to high accuracy over an extremely broad range of transmission factors. The ratio of the matrix attenuation for the set of shells to that of the VWA result calculated using a modified Parker form stays within a few percent of unity across a huge dynamic range of Transmission – larger than is practical to measure in routine use. This demonstrates that in the FFA at least, the 6 or 7 rod approach is excellent. To the extent that performing a uniform calibration is representative, then the rod approach is not only excellent approximation, but, also, is far easier than scanning a single point source. Relatively small correction factors, such as those tabulated, can be applied if needed to improve the overall accuracy of the calibration. The major effect identified in this work was the differential attenuation between the rod source assemblies and the displaced matrix material – especially at the lower transmission factors (highest drum densities). Again calculated corrections can be applied as needed although there is scope to alter to hole design to alleviate the problem to some extent.

REFERENCES

1. ASTM. Standard test method for nondestructive assay of special nuclear material in low-density scrap and waste by segmented passive gamma-ray scanning. ASTM C 1133-96 (1996)

2. S. Croft, R.D. McElroy, B.M. Young and R. Venkataraman; Quantifying SGS Matrix Correction Factor Uncertainties for Non-Uniform Source Distributions. Proceedings of 45th Annual Meeting of the INMM (Institute of Nuclear Materials Management'04), Paper 209, CD-ROM © 2004

3. G.C. Giesler, S.A. Henry, S.L. Johnson and D.W. Vehar; Calibration and characterisation of a low level waste assay system. Waste Management '94, Publ. Laser Options, Inc., Vol. 3 (1994) pp 2175-2179. Library of Congress No. 86-644175

4. J.H. Liang, S.H. Jiang and G.T. Chou; A theoretical investigation of calibration methods for radwaste radioactivity detection systems. Appl. Radiat. and Isot. 47(7) (1996) 669-675

5. M. Bruggeman, J. Gerits and R. Carchon; A minimum biased shell-source method for the calibration of rad waste assay systems. Appl. Radiat. and Isot. 51 (1999) 255-259

6. W. in der Schmitten, B. Sohnius and E. Wehner; Calculation of calibration factors and layout criteria for gamma scanning of waste drums from nuclear plants. Nucl. Technol. 92 (1990) 374-382

7. J.L. Parker, Attenuation Correction Procedures; Chap. 6 pp 159-194 In: Passive Nondestructive Assay of Nuclear Materials, D. Reilly, N. Ensslin, H. Smith, Jr., and S. Kreiner (Eds). United States Nuclear Regulatory Commission Report NUREG/CR-5550 (1991). Also Los Alamos National Laboratory Report LA-UR-90-732 (March, 1992). ISBN 0-16-032724-5

8. T.D. Reilly and J.L. Parker, Guide to gamma-ray assay for nuclear material accountability. Los Alamos National Laboratory Report: LA-5794-M (1975)

9. J.L. Parker and T.D. Reilly, Bulk sample self-attenuation correction by transmission measurement. Proc. ERDA X- and Gamma-Ray Symp. Ann Arbor, Michigan, May 19-21, 1976, pp 219-222 (Conf. 7606391)

10. J.K. Dickens, Self-absorption of gamma-rays produced in large cylindrical samples. Nucl. Instrum. Meths. 98 (1972) 451-454

11. M.J. Berger, J.H. Hubbell and S.M. Seltzer, XCOM: Photon cross sections database (1998). NIST standard reference database 8 (XGAM) NBSIR87-3597. Located at website: www.nndc.bnl.gov

12. R.B. Firestone and V.S. Shirley (Eds), Table of Isotopes 8th Edition Vol. II. John Wiley & Sons, Inc. (NY, 1996). ISBN 0-471-14917-9